An Efficient, Redox-Enhanced Pair of Hydrogen-Bond Tweezers for Chloride Anion Recognition, a Key Synthon in the Construction of a Novel Type of Organic Metal based on the Secondary Amide-Functionalized Ethylenedithiotetrathiafulvalene, β''-(EDT-TTF-CONHMe)$_2$[Cl·H$_2$O]

Karine Heuzé,[†] Cécile Mézière,[†] Marc Fourmigué,*[,†] Patrick Batail,*[,†] Claude Coulon,[‡] Enric Canadell,[§] Pascale Auban-Senzier,[||] and Denis Jérome[||]

Laboratoire Sciences Moléculaires aux Interfaces, FRE CNRS 2068, 2, rue de la Houssinière, 44322 Nantes Cedex 03, France; Centre de Recherches Paul Pascal (CRPP-CNRS), Av. Dr. Schweitzer, 33600 Pessac, France; Institut de Ciència de Materials de Barcelona (CSIC), Campus de la UAB, E-08193 Bellaterra, Spain; and Laboratoire de Physique des Solides, Bât. 510, Université Paris-Sud, 91405 Orsay Cedex, France

Received February 18, 2000

Electrocrystallization of 1,1,2-trichloroethane solutions of the redox-active secondary amide, 3-methylamido-3′,4′-ethylenedithiotetrathiafulvalene (EDT-TTF-CONHMe **1**) in the presence of *n*-Bu$_4$NF supported on silica gel afforded a mixed-valence chloride salt, formulated (**1**)$_2$-[Cl·H$_2$O] from elemental analysis and X-ray crystal structure resolution. The chloride anion and water molecule are disordered on the same site, and coordinated to the π-donor molecule by two strong hydrogen bonds involving the amidic N−H and the aromatic C−H group ortho to the amide, thereby qualifying a robust pair of tweezers-like cyclic motif. This efficient anion recognition effect is also observed in solution, as demonstrated by ^{1}H NMR downfield shifts of both the N−H and C−H hydrogen atom resonances, as well as by a cathodic shift of the oxidation potential of **1** upon Cl$^-$ complexation, establishing that the actual electrocrystallized species is a solvated anionic chloride complex [(**1**·Cl$^-$)(H$_2$O)$_n$] rather than the free amide. (**1**)$_2$[Cl·H$_2$O] adopts a layered β''-type structure with segregation of the hydrophobic (EDT-TTF) and hydrophilic (amide, Cl$^-$, H$_2$O) fragments. The HOMO−HOMO intermolecular interaction energies for the donor layers are large and the Fermi surface exhibits a pronounced two-dimensional character. The EPR Dysonian line observed below 120 K indicates an highly conducting system, confirmed by high room-temperature conductivity of 120 S cm^{-1} and metallic behavior down to 0.47 K, with a 167-fold increase of the conductivity, but no indication however of a transition to a superconducting state, a likely consequence of the Cl$^-$/H$_2$O disorder.

Introduction

The energy gain upon formation of partially occupied conduction bands in mixed-valence metallic and superconducting molecular cation radical salts[1] is balanced by the competing stabilization energies of collections of weaker intermolecular interactions, the most prominent being van der Waals interactions and C−H···X hydrogen bonds.[2,3] This delicate and complex balance ultimately dictates the pattern of intermolecular overlap within conducting chains or slabs and, as a consequence, their collective and transport properties.[4] It is therefore highly desirable to direct the formation of extended motifs by attaching to the redox π-system functionalities able to promote hydrogen bonds, halogen−halogen or halogen−nitrogen interactions,[5] which also provide a path for donor−donor or donor−anion electronic conjugation.[6] A number of tetrathiafulvalenes (TTFs) have been functionalized with −OH or −NH substituents but

[†] Laboratoire Sciences Moléculaires aux Interfaces.
[‡] Centre de Recherches Paul Pascal.
[§] Institut de Ciència de Materials de Barcelona.
[||] Laboratoire de Physique des Solides.

(1) Williams, J. M.; Ferraro, J. R.; Thorn, R. J.; Carlson, K. D.; Geiser, U.; Wang, H. H.; Kini, A. M.; Whangbo, M.-H. In *Organic Superconductors (Including Fullerenes)*; Prentice Hall: Engelwood Cliffs, NJ, 1992.

(2) Whangbo, M.-H.; Jung, D.; Ren, J.; Evain, M.; Novoa, J. J.; Mota, F.; Alvarez, S.; Williams, J. M.; Beno, M. A.; Kini, M. A.; Wang, H. H.; Ferraro, J. R. In *The Physics and Chemistry of Organic Superconductors*; Saito, G., Kagoshima, S., Eds.; Springer-Verlag: Heidelberg, Germany, 1990; p 262. (b) Davidson, A.; Boubekeur, K.; Pénicaud, A.; Auban, P.; Lenoir, C.; Batail, P.; Hervé, G. *J. Chem. Soc. Chem. Commun.* **1989**, 1373.

(3) Pénicaud, A.; Boubekeur, K.; Batail, P.; Canadell, E.; Auban-Senzier, P.; Jérome, D. *J. Am. Chem. Soc.* **1993**, *115*, 4101. (b) Schlueter, J. A.; Williams, J. M.; Geiser, U.; Dudek, J. D.; Kelly, M. E.; Sirchio, S. A.; Carlson, K. D.; Naumann, D.; Roy, T.; Campana, C. F. *Adv. Mater.* **1995**, *7*, 634.

(4) Batail, P.; Fourmigué, M. *Acc. Chem. Res.* to be submitted.

(5) Desiraju, G. R. *Angew. Chem., Int. Ed. Engl.* **1995**, *34*, 2311−2327.

(6) Figgis, B. N.; Kucharski, E. S.; Vrtis, M. *J. Am. Chem. Soc.* **1993**, *115*, 176.

10.1021/cm000143k CCC: $19.00
Published on Web 06/13/2000

only a few were engaged as single crystals of cation radical salts,[4,7] which ultimately proved to be either 1:1 Mott insulators or 2:1 semiconductors. We recently prepared amide-functionalized ethylenedithiotetrathiafulvalenes, EDT-TTF-$CONR_2$ (R = H, Me), explored their crystal chemistry,[8] and constructed two cation radical salts of the primary amide, $(EDT\text{-}TTF\text{-}CONH_2)_6AsF_6$ and $(EDT\text{-}TTF\text{-}CONH_2)_2ReO_4$, where N—H···O(F) and C—H···O hydrogen bonds were shown to cooperate, effectively discriminate between the different anion symmetries and afford vastly different architectures and collective properties.[9] Here, we report on the title compound, the first salt of the secondary amide EDT-TTF-CONHMe **1**, a water solvate where combined strong N—H···Cl/O and C—H···Cl/O hydrogen bonds and efficient overlap interactions both contribute to the stabilization of a layered structure which exhibits metallic character down to low temperature.

The combination of an activated hydrogen atom ortho to an amide function yields a robust, tweezers-like hydrogen-bonded seven-membered ring motif revealed herein and underscores its potential for efficient small anion recognition, in solution as well as in the solid state.

Results and Discussion

Solid-State Studies Reveal a Robust Pair of Hydrogen-Bond Tweezers Which Promotes the Chloride Anion Recognition Process. 1 was prepared as previously described[8] from the corresponding methyl ester via the acid and the acid chloride. Its first oxidation potential, observed at 0.50 V vs SCE is intermediate between values determined for EDT-TTF (0.44 V vs SCE) and BEDT-TTF (0.56 V vs SCE) in the same conditions and the small anodic shift found when compared with EDT-TTF, is attributable to the electron-withdrawing amide substituent. Early electrocrystallization experiments in the presence of a variety of anions (AsF_6^-, ReO_4^-, Cl^-, Br^-, etc.) afforded very small crystals only. In an attempt to form the fluoride salt **1** was electrocrystallized in 1,1,2-trichloroethane in the presence of n-Bu_4NF supported on silica gel. Black platelike crystals were harvested on the anode after 2 weeks. Microprobe analysis revealed that a chloride anion had been included instead of a fluoride anion, with 0.8 Cl atom for 12 S atoms, i.e., slightly less than one Cl^- for two EDT-TTF-CONHMe molecules. These Cl^- anions most probably originate from the decomposition of the chlorinated solvent, as already reported by Shibaeva et al.,[10] Day et al.,[11] and Mori et al.[12] upon electrocrystallization of BEDT-TTF salts. In a control experiment, electrocrystallization of BEDT-TTF carried out in similar conditions yielded high-quality single crystals of $(BEDT\text{-}TTF)_3Cl_2\cdot H_2O$, whose crystal structure and the occurrence of a metal-to-insulator transition at 100 K, unambiguously demonstrate that this phase is identical to that described earlier.[10,11] The fluoride anions introduced with n-Bu_4NF supported on silica gel then appear to strongly activate the chlorinated solvents,[13] affording an efficient, low-concentration chloride anion source in electrocrystallization experiments. Note also that attempts to electrocrystallize EDT-TTF-CONHMe in the presence of PPh_4Cl as a alternative chloride source afforded also the title compound, albeit of poorer crystalline quality.

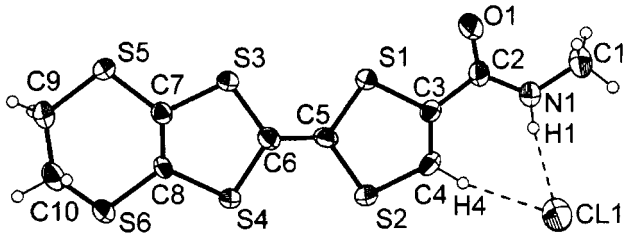

Figure 1. The asymmetric unit for $(\mathbf{1})_2Cl\cdot H_2O$ (ORTEP, probability level 50%), exemplifying the pair of hydrogen-bond tweezers promoting the chloride anion recognition process.

Table 1. Important Bond Distances within the TTF Core in $(\mathbf{1})_2Cl\cdot H_2O$ and in the Neutral 1 Molecule

	$(\mathbf{1})_2Cl\cdot H_2O$	$\mathbf{1}^a$
N1−C1	1.446(6)	1.438(5)
N1−C2	1.328(6)	1.333(20)
O1−C2	1.219(5)	1.236(7)
C2−C3	1.491(6)	1.482(6)
C3−C4	1.331(6)	1.322(8)
S1−C3	1.746(5)	1.752(8)
S1−C5	1.748(4)	1.761(5)
S2−C4	1.720(5)	1.717(4)
S2−C5	1.748(4)	1.757(4)
C5−C6	1.338(5)	1.331(6)
S3−C6	1.731(5)	1.758(5)
S3−C7	1.741(5)	1.746(9)
S4−C6	1.747(4)	1.760(5)
S4−C8	1.741(5)	1.742(9)
C7−C8	1.344(6)	1.323(6)

[a] Bond lengths of the two crystallographically independent molecules in the neutral **1** have been averaged and the given esd are the largest of the two values: (i) the individual esd, (ii) the standard deviations calculated as $\sigma(d_{mean}) = [\Sigma(d_i - d_{mean})^2/(n+1)]^{1/2}$. The numbering for $\mathbf{1}^{+0.5}$ in $(\mathbf{1})_2Cl\cdot H_2O$ has been used here for the neutral **1** instead of the original one.

The X-ray crystal structure determination reveals that both the donor molecule and the anion are located in general position in the unit cell (Figure 1). Comparison of bond lengths within the TTF core with those of the neutral donor molecule[8] (Table 1) confirms the oxidized character of the donor, as shown by the lengthening of the C=C double bonds, the concurrent shortening of the C−S bonds and the reinforcement of the planarity of the TTF donor core. The electronic conjugation of the amidic moiety with the dithiole ring is demonstrated by the shortening of S2−C4 relative to S1−C3, as observed previously in the neutral form **1**.[8]

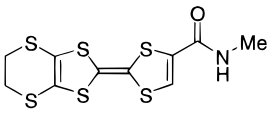

EDT-TTF-CONHMe (**1**)

Also, the amide adopts a trans configuration where both the hydrogen atoms of the N−H and the neighboring

(7) Bryce, M. R. *J. Mater. Chem.* **1995**, *5*, 1481.
(8) Heuzé, K.; Fourmigué, M.; Batail, P. *J. Mater. Chem.* **1999**, *9*, 2373.
(9) Heuzé, K.; Fourmigué, M.; Batail, P.; Canadell, E.; Auban-Senzier, P. *Chem. Eur. J.* **1999**, *5*, 2971.
(10) Shibaeva, R. P.; Lobkovskaya, R. M.; Rozenberg, L. P.; Buravov, L. I.; Ignatiev, A. A.; Kushch, N. D.; Laukhina, E. E.; Makova, M. K.; Yagubskii, E. B.; Zvarykina, A. V. *Synth. Met.* **1988**, *27*, A189.
(11) Rosseinsky, M. J.; Kurmoo, M.; Talham; D. R.; Day, P.; Chasseau, D.; Watkin, D. *J. Chem. Soc. Chem. Commun.* **1988**, 88.
(12) Mori, T.; Inokuchi, H. *Chem. Lett.* **1987**, 1657.
(13) Clark; J. H. *Chem. Rev.* **1980**, *80*, 429.

Table 2. Geometrical Characteristics of the N—H···Cl/O and C—H···Cl/O Hydrogen Bonds in $(1)_2Cl{\cdot}H_2O$

D—H···A	D···A dist (Å)	H···A dist (Å)	D—H···A ang (deg)
N1—H1···(Cl1/O2)	3.325(9)	2.479(9)	168.0(1)
C4—H4···(Cl1/O2)	3.42(1)	2.52(1)	167.2(2)

C—H point toward the chloride site. Refinement of the occupation parameter of the Cl^- site converged to 0.72. This result, together with the former microprobe analysis data led us to consider substitutional disorder involving a water molecule, i.e., with a Cl^-/H_2O ratio close to 50:50. Refinement on this single site of the occupation parameters of the chloride and oxygen atoms with identical thermal parameters, converged to 0.60 and 0.40 respectively, when the microprobe data yielded the opposite, 40:60 ratio instead. It is not unlikely that the actual chloride-to-water proportion may vary from one crystal to the other. This type of substitutional disorder has been encountered previously, for example in quaternary ammonium clathrate hydrates where chloride ions readily substitute for water molecules[14] as well as in the chloride salt of BEDO-TTF, formulated $(BEDO\text{-}TTF)_2Cl_{1.28}(H_3O)_{0.28}{\cdot}2.44H_2O$.[15] Hence the proposed title formulation, $(EDT\text{-}TTF\text{-}CONHMe)_2[Cl{\cdot}H_2O]$, i.e., with an averaged 2:1 stoichiometry.

As exemplified in Figure 1, a robust hydrogen-bond motif is identified in the solid-state structure, that is, the pair of hydrogen-bond tweezers captures as many water molecules as chloride anions via the NH group of the amidic moiety and the CH group of the EDT-TTF core, ortho to the conjugated amidic function. The geometrical characteristics of these hydrogen bonds, collected in Table 2, show that the N1—H1···(Cl/O) bond lengths lie in the expected ranges for N—H···O[16] or N—H···Cl[17] hydrogen bonds. The C4—H4···(Cl/O) hydrogen bond is particularly short and close to linear,[18,19] an indication of strong bonding, and a likely consequence of the combined effects of the ortho electron-attracting amidic group and of the cationic state of the EDT-TTF core. A closer look at the structure of the 1:1 and insulating, secondary TTF thioamide salt (TTF-CSNHMe)(Br) reported recently by Bryce et al.,[20] and for which only the occurrence of the N—H···Br^- hydrogen bond was mentioned, also reveals a similar C—H···Br^- hydrogen bond and the occurrence of a similar tweezers-like motif. The present results provide growing evidence of the potential of the amidic function in the recognition of small anions,[21] as exemplified by recent studies by Beer et al. on halide salts of cationic colbatocinium-,[22] or metal bipyridyl-based[23] secondary amides whose structures show that the coordinated chloride anions are systematically engaged in the expected N—H···Cl^- but also in C—H···Cl^- hydrogen bonds with the hydrogen atom of the aromatic moiety (Cp, bipy) bearing the amidic group. It is interesting to note that the novel supramolecular synthon identified here possess all the attributes of a robust crystal engineering principle, especially in the sense where the repetitive unit can be readily deciphered in the compound formulation itself.[24]

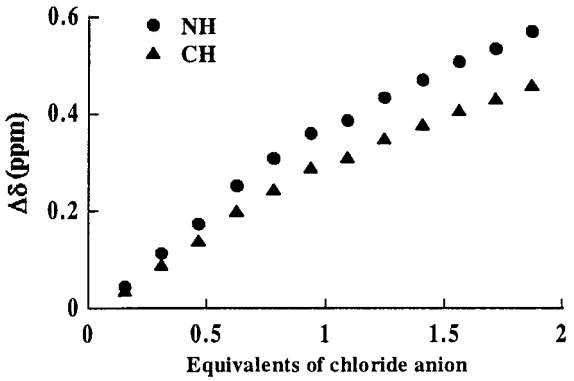

Figure 2. ^1H NMR titration curves of **1** by successive amounts of Cl^- in d_6-DMSO solution.

The Pair of Hydrogen-Bond Tweezers Also Captures Chloride Anions in Solution. Following up on the former crystal chemistry evidence, this was first demonstrated by ^1H NMR titration experiments in which significant downfield shifts of the amidic proton resonance were recorded (Figure 2) upon addition of successive amounts of $n\text{-}Bu_4NCl$ to a d_6-DMSO solution of **1**. These shifts are comparable to those observed for the amidic proton resonance, in the presence of chloride anions, for a *cationic N*-butylamidocobaltocenium complex where electrostatic interactions are also expected to play a significant role in the complex stabilization. Note that the corresponding amidic proton resonance of *neutral* secondary amides have been reported to exhibit no such shift upon chloride addition.[22,25] Thus, the present results demonstrate that **1** binds chloride anions in solution stronger than other neutral aromatic amides. Of particular note is the parallel, significant downfield shift observed for the aromatic proton (H4) ortho to the amidic group (Figure 2). This confirms its involvement in the chloride anion binding via the C—H···Cl^- hydrogen bond. ^1H NMR titration data based on both the N—H and C—H chemical shift evolution for the equilibrium: $\mathbf{1} + Cl^- \leftrightarrow \mathbf{1}{\cdot}Cl^-$ yield a common value[26] of $K = [\mathbf{1}{\cdot}Cl^-]/([\mathbf{1}][Cl^-]) = 10\ dm^3\ mol^{-1}$, thus demonstrating that the complexing ability of neutral **1** originates in the cooperative effect of both N—H···Cl^-

(14) Jeffrey, G. A.; Saenger, W. In *Hydrogen Bonding in Biological Structures*; Springer: Berlin, 1991; Chapter 11.
(15) Shibaeva, R. P.; Khasanov, S. S.; Narymbetov, B. Z.; Zorina, L. V.; Rozenberg, L. P.; Bazhenov, A. V.; Kushch, N. D.; Yagubskii, E. B.; Rovira, C.; Canadell, E. *J. Mater. Chem.* **1998**, *8*, 1151.
(16) Taylor, R.; Kennard, O. *Acta Crystallogr. B* **1984**, *40*, 280.
(17) (a) Mascal, M. *J. Chem. Soc., Perkin Trans. 2* **1997**, 1999. (b) Steiner, T. *Acta Crystallogr.* **1998**, *B54*, 456.
(18) Desiraju, G. R. *Acc. Chem. Res.* **1991**, *24*, 290.
(19) Aakeröy, C. B.; Evans, T. A.; Seddon, K. R.; Palinko, I. *New. J. Chem.* **1999**, 145.
(20) The following geometrical characteristics are found for the N—H···Br hydrogen bond: d(H···Br) = 2.257 Å, ang(N—H···Br) = 157.2°; for the C—H···Br hydrogen bond: d(H···Br) = 2.680 Å, ang(C—H···Br) = 159°. Moore, A. J.; Bryce, M. R.; Batsanov, A. S.; Heaton, J. N.; Lehman, C. W.; Howard, J. A. K.; Roberstyon, N.; Underhill, A. E.; Perepichka, I. F. *J. Mater. Chem.* **1998**, *8*, 1541.
(21) Dietrich, B. *Pure Appl. Chem.* **1993**, *65*, 1457.
(22) (a) Beer, P. D.; Hesek, D.; Hodacova, J.; Stockes, S. E. *J. Chem. Soc., Chem. Commun.* **1992**, 270. (b) Beer, P. D.; Hesek, D.; Kingston, J. E.; Smith, D. K.; Stokes, S. E.; Drew, M. G. B. *Organometallics* **1995**, *14*, 3288. (c) Beer, P. D.; Drew, M. G. B.; Graydon, A. R.; Smith, D. K.; Stokes, S. E. *J. Chem. Soc. Dalton Trans.* **1995**, 403.
(23) Beer, P. D.; Dickson, C. A. P.; Fletcher, N.; Goulden, A. J.; Grieve, A.; Hodacova, J.; Wear, T. *J. Chem. Soc., Chem. Commun.* **1993**, 828.
(24) Desiraju, G. R.; Steiner, T. In *The Weak Hydrogen Bond*; Oxford University Press: Oxford, 1999.
(25) Valério, C.; Fillaut J.-L.; Ruiz, J.; Guittard, J.; Blais, J.-C.; Astruc, D. *J. Am. Chem. Soc.* **1997**, *119*, 2588.
(26) The program EQNMR was used to estimate the stability constants: Hynes, M. J. *J. Chem. Soc., Dalton Trans.* **1993**, 311.

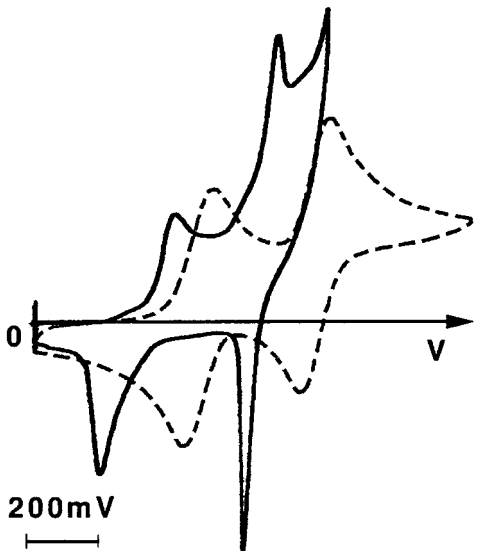

Figure 3. Cyclic voltamograms of CH_3CN solutions of **1** (vs SCE, *n*-Bu_4NPF_6 0.05 M) (dotted line) and of CH_3CN solutions of **1** with a 10-fold excess of *n*-Bu_4NCl (full line). Note, in the latter, the characteristic sharp return peaks indicating crystallization at the electrode during the anodic process.

and C—H···Cl^- hydrogen bonds, again qualifying the seven-membered ring motif disclosed herein.

The former results unambiguously demonstrate that in the presence of chloride anions, significant amounts of the anionic complex (**1**·Cl^-) are formed in solution in equilibrium with the free amide. Therefore, the electrooxidized species may not be the free amide **1** but, rather, the anionic complex (**1**·Cl^-) which, on account of its negative charge, is expected to oxidize at lower potentials. This is confirmed by cyclic voltammetry experiments (Figure 3) performed in the presence of a 10-fold excess of PPh_4Cl and showing that the oxidation potential of **1**, initially observed at 0.50 V vs SCE, is shifted by 110 mV toward more cathodic potentials. Note also that upon chloride addition, the cyclic voltamogram is strongly affected by precipitation processes at the electrode, as evidenced by the sharp peaks observed on the second oxidation and the two reduction processes. We then conclude that the species which crystallizes on the anode is likely to be the solvated, zwitterionic complex, ($\mathbf{1}^{+\bullet}$)[(Cl^-)·(H_2O)$_n$] rather than the free, oxidized amide $\mathbf{1}^{+\bullet}$.[27]

A Two-Dimensional Metal with an Unprecedented Architecture Akin to the β-Type. When collections of the former zwitterionic motif, ($\mathbf{1}^{+\bullet}$)[(Cl^-)·(H_2O)$_n$], assemble at the electrode, a neat partition of the hydrophilic and hydrophobic moieties occurs and drives the formation of the layered structure shown in Figure 4, a construction principle encountered earlier for the electrocrystallized neutral (zwitterionic) π-radical [Me_3-TTF-PO(OH)O^-]·$^+$.[28] Of particular note is the short separation (3.09(1) Å) between the inversion-related Cl^-/H_2O sites. This distance falls in the reported range for Cl···O distances between water or alcohol molecules hydrogen bonded to Cl^-.[10,14] This suggests that the chloride and water molecules may be locally ordered in any given site into Cl^-/H_2O or H_2O/Cl^- pairs stabilized by a O—H···Cl^- hydrogen bond, thereby also avoiding the close proximity of two negatively charged chloride anions. Thus, within this pattern, each chloride is three-coordinated, as observed most commonly.[14] The former hydrogen-bonded pairs and the extended cooperative (N/C)—H···O—H···Cl···H—(N/C) motif incorporating five hydrogen bonds which develops at the interface, serve to anchor the parallel organic slabs onto one another.

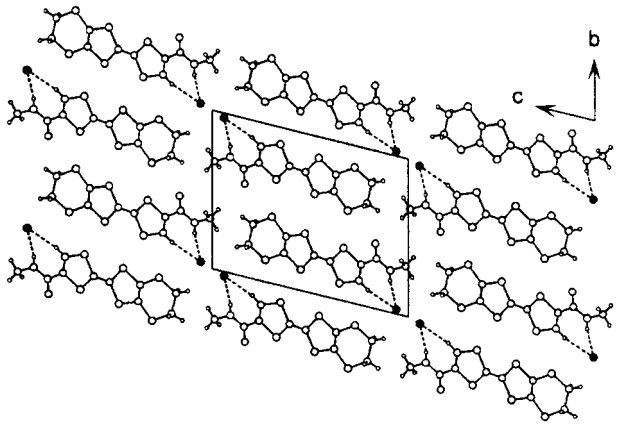

Figure 4. The partition of the hydrophilic and hydrophobic moieties into parallel slabs viewed down the [100] axis. The N—H···Cl/O and C—H···Cl/O hydrogen bonds are indicated by dotted lines.

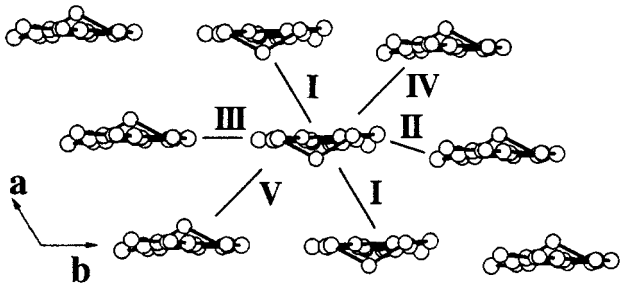

Figure 5. Pattern of intermolecular interactions within the conducting slab looking down the long molecular axis and emphasizing its relationship to the prototypical β''-topology. The HOMO−HOMO interaction energies (eV) read as follows: I, 0.3974; II, 0.1171; III, 0.2259; IV, 0.2550; V, 0.2216.

Within one slab, the molecules adopt the β''-type pattern[29] of intermolecular interactions shown in Figure 5. The calculated HOMO−HOMO intermolecular interaction energies, which are a measure of the strength of the interaction between two donor HOMOs in adjacent positions of the lattice, are quite large. Those along the stacks along *a* are comparable to those found in metallic salts of BEDT-TTF such as β-(BEDT-TTF)$_2(I_3)$, β-(BEDT-TTF)$_2(AuI_2)$, and β-(BEDT-TTF)$_2(IBr_2)$.[30] The interstack interactions are considerably larger in the present salt

(27) In that respect, these observations qualify the present model system for further in-depth studies of the electrocrystallization mechanism, focusing on the yet unsettled issue as to where the supramolecular association takes place, in solution prior to the actual crystallization, as suggested here, or directly at the crystal or electrode surface. For a review, see: Batail, P.; Boubekeur, K.; Fourmigue, M.; Gabriel, J.-C. P. *Chem. Mater.* **1998**, *10*, 3005−3015.

(28) Dolbecq, A.; Fourmigué, M.; Krebs, F. C.; Batail, P.; Canadell, E.; Clérac, R.; Coulon, C. *Chem. Eur. J.* **1996**, *2*, 1275.

(29) (a) Mori, T. *Bull. Chem. Soc. Jpn.* **1999**, *71*, 2509. (b) Kurmoo, M.; Graham, A. W.; Day, P.; Coles, S. J.; Hursthouse, M. B.; Caulfield, J. L.; Singleton, J.; Pratt, F. L.; Hayes, W.; Ducasse, L.; Guionneau, P. *J. Am. Chem. Soc.* **1995**, *117*, 12209. (c) Geiser, U.; Schlueter, J. A.; Wang, H. H.; Kini, A. M.; Williams, J. M.; Sche, P. P.; Zakowicz, H. I.; VanZile, M. L.; Dudek, J. D. *J. Am. Chem. Soc.* **1996**, *118*, 9996.

(30) Emge, T. J.; Wang, H. H.; Geiser, U.; Beno, M. A.; Webb, K. S.; Williams, J. M. *J. Am. Chem. Soc.* **1986**, *108*, 3849.

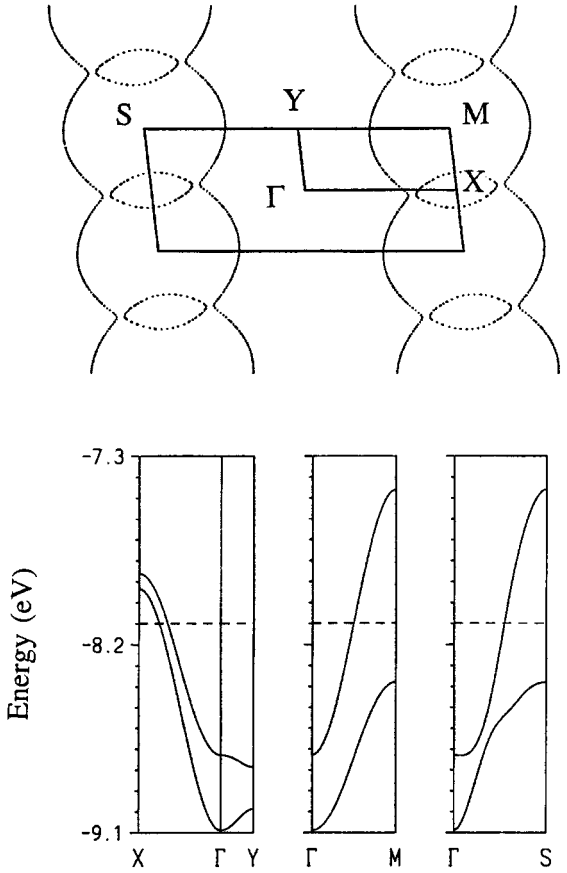

Figure 6. Electronic band structure (bottom) and Fermi surface (top) calculated for β''-(EDT-TTF-CONHMe)$_2$[Cl·H$_2$O]. The dotted line indicates the position of the Fermi level. Γ, X, Y, M and S refer to the (0,0), (a*/2, 0), (0,b*/2), (a*/2,b*/2), and (−a*/2,b*/2) wave vectors, respectively.

so that a strong 2D metallic character is anticipated. It is worth mentioning that there are short S···S contacts (between 3.44 and 3.69 Å) associated with interactions II−V. However, only S···S contacts as long as 3.95 Å are associated with interaction I which, in fact, leads to the strongest HOMO···HOMO interaction of the layer (see caption for Figure 5). As already discussed for the neutral π-radical [Me$_3$TTF-PO$_3$H$^-$]$^{+\bullet}$,[28] a system for which the HOMO bands exhibit a sizable dispersion despite the fact that there are practically no short S···S contacts in the layers, interaction I is associated here with very strong σ-type interactions between the S and C p orbitals which are nearly on top of each other. The calculated band structure for this β''-slab is given in Figure 6 together with the corresponding Fermi surface associated with a 2:1 stoichiometry, i.e., a $^3/_4$ filled system.[31] The two different molecular orientations of the donor molecule imply that there are two donors per repeat unit of the layer which give rise to two HOMO bands whose dispersion is large in the Γ-X and Γ-M sections but limited in the Γ-Y one. The conducting β-slab exhibits a Fermi surface (Figure 6) akin to that of a κ-phase, with the characteristic overlapping circular orbits reminiscent of those encountered for κ-(BEDT-TTF)$_2$Cu(NCS)$_2$ or κ-(BEDT-TTF)$_2$I$_3$,[32] despite the very different band structure and topology of the layers.

(31) The calculated Fermi surface does not differ substantially from that obtained with the 50:50 Cl$^-$/H$_2$O ratio if one considers alternative 60:40 or 40:60 values.

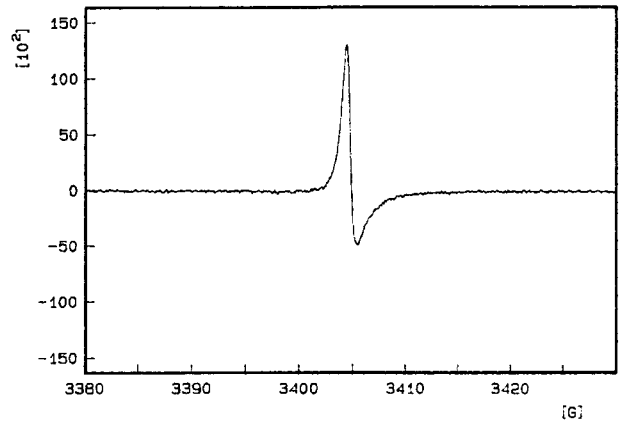

Figure 7. ESR spectrum of a single crystal of β''-(EDT-TTF-CONHMe)$_2$[Cl·H$_2$O] at 4 K.

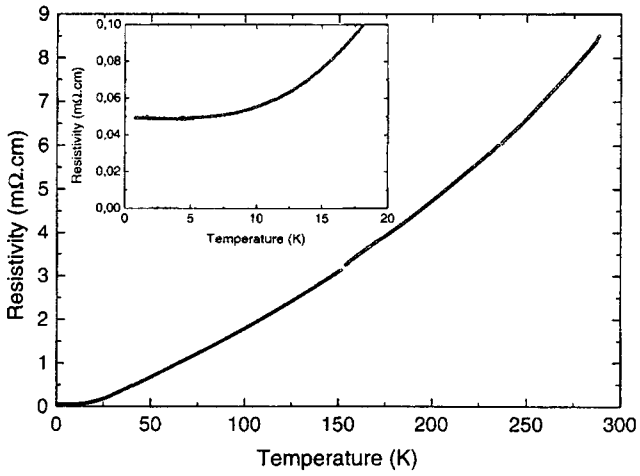

Figure 8. Resistivity down to 0.47 K of a single crystal of β''-(EDT-TTF-CONHMe)$_2$[Cl·H$_2$O].

From these results, which agree with the above qualitative analysis, one expects this salt to exhibit metallic conductivity, as indeed observed experimentally. The absence of any nesting properties in the Fermi surface suggests that no density wave type anomalies leading to the suppression of the metallic state will be found when lowering the temperature. EPR measurements performed on an oriented single crystal between 300 and 4 K show a single line in the whole temperature range. The deduced spin susceptibility is essentially temperature independent, as expected for a Pauli-type behavior. Below 110 K, the resonance line becomes strongly asymmetric (Figure 7), the signature of a so-called Dysonian line,[33,34] characteristic of a highly conducting system and which has been observed previously for a few BEDT-TTF salts.[35] As shown in Figure 8, the room-temperature conductivity amounts to 120 S cm^{-1} and the system remains metallic down to 0.47 K where a 167-fold increase of the conductivity has occurred at this

(32) Jung, D.; Evain, M.; Novoa, J. J.; Whangbo, M.-H.; Beno, M. A.; Kini, A. M.; Schultz, A. J.; Williams, J. M.; Nigrey, P. J. *Inorg. Chem.* **1989**, *28*, 4516.

(33) Pifer, J. H.; Magno, R. *Phys. Rev. B* **1971**, *3*, 663.

(34) (a) Feher, G.; Kip, A. F. *Phys. Rev.* **1955**, *98*, 337. (b) Dyson, F. J. *Phys. Rev.* **1955**, *98*, 349.

(35) (a) Wang, H. H.; Carlson, K. D.; Geiser, U.; Kwok, W. K.; Vashon, M. D.; Thompson, J. E.; Larsen, N. F.; McCabe, G. D.; Hulscher, R. S.; Williams, J. M. *Physica C* **1990**, *166*, 57. (b) Venturini, E. L.; Azevedo, L. J.; Schirber, J. E.; Williams, J. M.; Wang H. H., *Phys. Rev. B* **1985**, *B32*, 2819. (c).

temperature (Figure 8). The failure to observe a transition to a superconducting state may be due to the occurrence of disorder on the anion site in the vicinity of the metallic slab. This was postulated earlier for β-(BEDT-TTF)$_2$I$_2$Br where the I_2Br^- anion is found disordered on an inversion center,[36] while the isostructural salts with centrosymmetrical anions, β-(BEDT-TTF)$_2$I$_3$ and β-(BEDT-TTF)$_2$IBr$_2$ are both superconducting. Attempts to suppress this disorder by introducing on the Cl^-/H_2O sites a centrosymmetrical anion of comparable length are now being explored, for example by engaging the linear N_3^- or HCl_2^- anions, which are also expected to enter in the construction of a similar extended hydrogen-bond motif involving both the NH and the CH groups of the redox secondary amide at the slabs interface.

In conclusion, we have disclosed a novel robust supramolecular synthon based on a pair of tweezers-like hydrogen-bonded seven-membered ring motif involving both N—H···Cl/O and C—H···Cl/O hydrogen bonds and highlighted the capacity of the tetrathiafulvalenyl protons to enter in hydrogen-bond patterns. In addition, we have demonstrated that the chloride anion recognition process revealed in the solid-state preexists in solution, where the oxidation potential of the molecular complex [**1**·$Cl^-(H_2O)_n$] is effectively lowered vis-à-vis that of the discrete molecule, and provided strong evidence that the radical cation/anion association occurs in solution during the electrocrystallization process prior to the actual crystallization at the electrode. The unprecedented architecture of the highly conducting 2D metal, β-(EDT-TTF-CONHMe)$_2$[Cl·H_2O] is characterized by locally ordered Cl/H_2O pairs and a κ-phase-like Fermi surface. The system remains metallic with no convincing evidence for a superconducting transition at low temperature, a likely manifestation of the absence of long-range correlation between the former pairs, a typical example of the role of disorder in molecular conductors.

Experimental Section

Instrumentation. Nuclear magnetic resonance spectra were obtained on a Bruker AC200 instrument using the solvent deuterium signal as internal reference. Electrochemical measurements were carried out using an EGG PAR273 scanning potentiostat with a Pt working electrode (diameter = 1 mm) and a saturated calomel electrode (SCE) as reference. Microprobe analyses were performed on a CAMECA SX50 at the IFREMER (Brest, France). The ESR spectra were recorded on oriented single crystals on a Bruker ESP300E spectrometer equipped with a ESR900 cryostat (4.2−300 K) from Oxford Instruments. Magnetic susceptibility measurements were performed on a Quantum Design MPMS-2 SQUID magnetometer operating at 5000 G in the range 5−300 K. Elemental analysis were performed at the Institut de Chimie des Substances Naturelles, CNRS, Gif/Yvette.

Electrochemistry. Cyclic voltammetry experiments were performed in dry CH_3CN at 20 °C at a scan rate of 100 mV $s^{-1}$with n-Bu_4NPF_6 0.1 M as electrolyte. For the Cl^- complexation experiments, weighted amounts of solid PPh_4Cl were added in fractions to the cell and the solution was well stirred before a novel voltamogram was collected. Electrocrystallization of **1** was performed in a two-compartment cell with freshly distilled 1,1,2-trichloroethane (12 mL) and n-Bu_4NF adsorbed on silica gel (25 mg, Aldrich) with **1** (5 mg) in the anodic compartment only. Galvanostatic electrolysis at 0.4 μA during 14 days at 20 °C afforded platelike crystals on the anode. Anal. Calcd for (**1**)$_2$Cl·H_2O ($C_{20}H_{20}Cl_1N_2O_3S_{12}$): C, 31.75; Cl, 4.69; S, 50.86. Found: C, 31.74; Cl, 5.39; S, 50.37. Using the same conditions with BEDT-TTF (5 mg) as donor, at 0.5 μA and 30 °C afforded the 3:2 [BEDT-TTF]$_3Cl_2$ phase described by Shibaeva et al.[10] and Day et al.[11]

Table 3. Crystal Data and Structure Refinement for (1)$_2$[Cl·H_2O]

empirical formula	$C_{10}H_9Cl_{0.5}N\ O_{1.5}S_6$
formula weight	377.27
T (K)	293
radiation, wavelength (Å)	Mo Kα, $\lambda = 0.71073$
crystal system	Triclinic
space group	$P\bar{1}$
a (Å)	4.5376(6)
b (Å)	11.4249(14)
c (Å)	14.7464(19)
α (deg)	75.60(1)
β (deg)	83.88(1)
γ (deg)	83.05(1)
V (Å^3)	732.7(2)
Z	2
ρ_{calc} (g cm^{-3})	1.710
μ (Mo Ka) (mm^{-1})	1.015
F(000)	385
crystal size (mm)	0.28 × 0.06 × 0.02
crystal shape, color	plate, black
θ range (deg)	1.85, 25.83
completeness to $\theta = 25.83$	0.931
index ranges	$-5 \leqslant h \leqslant 5$, $-13 \leqslant k \leqslant 13$, $-17 \leqslant l \leqslant 18$
no of data collected	7142
no of unique data	2641 ($R_{int} = 0.1022$)
no reflections $I > 2\sigma(I)$	1249
max and min transmission	0.9710, 0.8728
refinement method	full-matrix least-squares on F^2
data/restraints/parameters	2641/0/174
goodness-of-fit on F^2	0.772
final R indices [$I > 2\sigma(I)$]	$R_1 = 0.0446$, w$R_2 = 0.0554$
R indices (all data)	$R_1 = 0.1265$, w$R_2 = 0.0668$
largest diff peak/hole (e Å^{-3})	0.290 and −0.293

X-ray Crystallography. Crystallographic data were collected at 293 K on a Stoe imaging plate diffraction system (IPDS) using graphite-monochromatized Mo Kα. The individual frames were measured with a φ oscillation of 1.6° and an acquisition time of 10 mn per frame. The Stoe IPDS software was used for data collection and reduction. Numerical absorption correction (FACEIT) using crystal faces was used. The complete data collection and refinement parameters are given in Table 3. The structure was solved using direct methods (SHELX86) and refined using SHELXL. All atoms except hydrogen atoms were refined anisotropically. Occupation parameter of the Cl/O site was refined while imposing a common agitation factor for both atoms. Hydrogen atoms were introduced at calculated positions (riding model) and not refined.

Band Structure Calculations. The tight-binding band structure calculations[37] were of the extended Hückel type.[38] A modified Wolfsberg-Helmholtz formula was used to calculate the nondiagonal $H_{\mu\nu}$ values.[39] Double-ζ orbitals for C, N, O, and S were used. The exponents and parameters for C, N, O, S, and H were taken from previous work.[28,40] The values

(36) Emge, T. J.; Wang, H. H.; Beno, M. A.; Leung, P. C. W.; Firestone, M. A.; Jenkins, H. C.; Cook, J. D.; Carlson, K. D.; Williams, J. M.; Venturini, E. L.; Azevedo, L. J.; Schriber, J. E. *Inorg. Chem.* **1985**, *24*, 1736.

(37) Whangbo, M.-H.; Hoffmann, R. *J. Am. Chem. Soc.* **1978**, *100*, 6093.

(38) Hoffmann, R. *J. Chem. Phys.* **1963**, *39*, 1397.

(39) Ammeter, J. H.; Bürgi, H.-B.; Thibeault, J.; Hoffmann, R. *J. Am. Chem. Soc.* **1978**, *100*, 3686.

employed for N were as follows: 2.261, 1.424, 0.7297, 0.3455, and −26.0 eV for N 2s, 3.249, 1.499, 0.2881, 0.7783, and −13.4 eV for N 2p.

Acknowledgment. We thank Y. Moëlo (IMN, Nantes) and M. Bohn (IFREMER, Brest) for the microprobe analysis. Financial support from the CNRS, the Ministry of Education (to H.K.), the Région Pays de la Loire, the DGES-Spain (project PB96-0859) and Generalitat de Catalunya (1997 SGR 24) is gratefully acknowledged.

(40) Dolbecq, A.; Boubekeur, K.; Batail, P.; Canadell, E.; Auban-Senzier, P.; Coulon, C.; Lerstrup, K.; Bechgaard, K. *J. Mater. Chem.* **1995**, *5*, 1707.

Supporting Information Available: An X-ray crystallographic file (CIF). This material is available free of charge via the Internet at http://pubs.acs.org.

CM000143K